

SLAC-PUB-842
November 1970

RECENT DEVELOPMENTS IN INELASTIC ELECTRON-NUCLEON SCATTERING*

Frederick J. Gilman

Stanford Linear Accelerator Center, Stanford University, Stanford, California 94305

Invited talk presented at the
Symposium on Hadron Spectroscopy
Balatonfüred, Hungary
September 6-11, 1970

* Work supported by the U. S. Atomic Energy Commission.

High energy inelastic electron-nucleon scattering probes the instantaneous charge distribution of the nucleon and provides a method for investigating possible substructure. In the year that has passed since the International Symposium on Electron and Photon Interactions at High Energies at Liverpool, a number of important developments have taken place in both the experimental and theoretical aspects of inelastic electron-nucleon scattering.¹ The Kiev conference has, in particular, seen the discussion of a large amount of new data from SLAC, including data on both electron-proton and electron-neutron inelastic scattering.² I propose to discuss here these developments, with particular attention to some theoretical consequences of the recent experimental data and to recent work on duality and resonance behavior. A discussion of other aspects of inelastic lepton-hadron scattering and related processes can be found in the proceedings of the Liverpool Symposium and the more recent Naples meeting.³

The process of inelastic electron-nucleon scattering is shown in Figure 1 where an electron (with energy E) is incident on a nucleon (of four-momentum P) and scatters (with resulting final energy E') by an angle θ due to the exchange of a single photon (of four-momentum q). If we do not observe the hadronic final state, as is the case in most of the experiments done until very recently, then the double differential cross section can be written as

$$\frac{d^2\sigma}{d\Omega'dE'} = \frac{4\alpha^2 E'^2}{q^4} \left[2W_1(\nu, q^2) \sin^2 \frac{\theta}{2} + W_2(\nu, q^2) \cos^2 \frac{\theta}{2} \right], \quad (1)$$

where the structure functions W_1 and W_2 depend on the two (Lorentz scalar) variables $\nu = -q \cdot P / M_N$ and q^2 , which can be written in terms of laboratory quantities

as (neglecting the lepton mass)

$$\begin{aligned} \nu &= E - E' \\ q^2 &= 4EE' \sin^2 \frac{\theta}{2} . \end{aligned} \quad (2)$$

If we know ν and q^2 (from measuring the incident and scattered electron) then the invariant mass W of the final hadrons is fixed by

$$s = W^2 = 2M_N \nu + M_N^2 - q^2 . \quad (3)$$

The structure functions W_1 and W_2 that appear in Eq. (1) arise from the quantity

$$\begin{aligned} W_{\mu\nu} &\equiv \frac{1}{4\pi\alpha} \sum_n \langle P | J_\mu^{(em)}(0) | n \rangle \langle n | J_\nu^{(em)}(0) | P \rangle (2\pi)^3 \delta^{(4)}(P_n - P - q) \\ &\equiv W_1(\nu, q^2) \left[\delta_{\mu\nu} - q_\mu q_\nu / q^2 \right] + W_2(\nu, q^2) \left[(P_\mu - P \cdot q q_\nu / q^2) (P_\nu - P \cdot q q_\mu / q^2) \right] / M_N^2 , \end{aligned} \quad (4)$$

which is just $(1/4\pi^2\alpha)$ times the imaginary part of the Feynman amplitude for forward Compton scattering of photons of mass² = $-q^2$. Since the optical theorem relates the imaginary part of the forward elastic amplitude to the total cross section, it is no surprise that one can also define⁴ total virtual photon-nucleon cross sections for transversely and longitudinally polarized photons, σ_T and σ_S , which are related to W_1 and W_2 and can be used instead of them to describe the results of inelastic electron-nucleon experiments. The relation of W_1 and W_2 to σ_T and σ_S is

$$W_1 = \frac{K}{4\pi^2 \alpha} \sigma_T$$

$$W_2 = \frac{K}{4\pi^2 \alpha} \frac{q^2}{q^2 + \nu^2} (\sigma_T + \sigma_S) . \quad (5)$$

where $K = \nu - q^2/2M_N = (W^2 - M_N^2)/(2M_N)$. Kinematic constraints force σ_S to vanish at $q^2 = 0$, while σ_T at $q^2 = 0$ is just the total photoabsorption cross section for real photons.

Although the kinematics certainly are straightforward and contain no surprises, the experiments on inelastic electron-nucleon scattering have yielded one surprise after another. First was its large size. This size may be simply summarized as being roughly point-like: When the cross section at fixed q^2 is integrated over ν one obtains a result which is the same order of magnitude as the Mott cross section for scattering from a point proton.

The same measurements which showed the point-like size of the scattering also showed a second phenomenon, the scaling behavior proposed by Bjorken⁵. "Scaling" is the statement that as ν and $q^2 \rightarrow \infty$, νW_2 and W_1 become non-trivial functions of the dimensionless ratio $\omega = 2M_N \nu/q^2$ only, rather than functions of both ν and q^2 as would be the case a priori. We may look for the scaling behavior in the data where ν and q^2 are finite by studying the behavior of νW_2 and W_1 at any fixed value of ω as we vary q^2 (and therefore ν) and see if they tend to (non-zero) limiting values as q^2 becomes large. An example of this for νW_2 at $\omega = 4$ is shown in Figure 2, where νW_2 is seen to have the same value over almost a decade of values of q^2 . It is worth emphasizing here that since scaling is a statement of behavior as ν and $q^2 \rightarrow \infty$, any other dimensionless variable, ω' , such that $\omega' \rightarrow \omega$ as

ν and $q^2 \rightarrow \infty$ is, in principle, just as suitable as ω for studying the scaling behavior of the data. Another variable could in fact lead to the scaling behavior sooner in the sense that νW_2 and W_1 could become independent of q^2 (and hence equal to their $q^2 \rightarrow \infty$ limit) for smaller values of q^2 if they are studied as functions of q^2 at fixed ω' rather than ω . This in fact appears to be the case for inelastic electron-proton scattering where the variable^{2,6}

$$\omega' = 1 + s/q^2 = \omega + M_N^2/q^2 \quad (6)$$

results, particularly for $1 < \omega < 4$, in a more rapid approach to the scaling behavior. This can be seen in Figures 3 and 4 where we have νW_2 plotted versus ω and ω' for various values of q^2 (all corresponding to $W \geq 2$ GeV so that we stay away from the prominent N^* resonances) and it is clear that νW_2 is more independent of q^2 for smaller values of q^2 when plotted versus ω' . In particular, we can see from Figure 3, that νW_2 decreases toward its asymptotic value as q^2 increases for fixed ω in the range $1 < \omega < 4$. Figure 4 shows that νW_2 scales (i. e., is a function of ω' only) to within the accuracy of the data for ω' in the range $1 < \omega' < 10$ as long as $q^2 \geq 1 \text{ GeV}^2$ and $W > 2 \text{ GeV}$. Such a small value of q^2 for the onset of scaling is rather remarkable.

In our discussion of scaling and plots of νW_2 we have used a third experimental finding, namely that $R = \sigma_S/\sigma_T$ is small and does not depend strongly on ν , q^2 , or ω . The knowledge of R is equivalent to being able to explicitly separate the contributions of W_1 and W_2 to the double differential cross section, Eq. (1). This separation is accomplished by measuring scattering (or interpolating from measurements) at different angles, but the same values of ν and q^2 , and has been reported² in some detail at Kiev. The value of R obtained by averaging over the 23 interpolated points between ω of 1 and 10 is 0.18 ± 0.05 . This is certainly small, and

given the possible systematic errors it is possible, although unlikely, that $R = 0$. In any case, it is now possible to plot W_1 and νW_2 at places where the separation has been made and roughly verify the scaling behavior for both W_1 and νW_2 . Alternately, one can choose a constant (or some other functional form) for R which is consistent with the data, and plot νW_2 and W_1 for all the data points, as we have done above for νW_2 . Such plots are consistent with both νW_2 and W_1 scaling for $1 < \omega' < 10$ (again, as long as $q^2 > 1 \text{ GeV}^2$ and $W > 2 \text{ GeV}$).

Some of the most exciting new data concerns the inelastic electron scattering off deuterium which allows deduction of inelastic electron-neutron cross sections. Neglecting corrections for internal motion, final state interactions, and Glauber corrections, which should all be small, then the neutron cross sections are given by the difference of the deuterium and hydrogen cross sections. Assuming that the ratio of longitudinal to transverse cross sections (or $W_1/\nu W_2$) is the same for the neutron and proton, then $\nu W_{2n}/\nu W_{2p} = D/H - 1$. This quantity is shown in Figure 5 plotted versus ω .⁷ Clearly $\nu W_{2n}/\nu W_{2p}$ is smaller than unity in the range $1.5 < \omega < 6$ and further, $\nu W_{2n}/\nu W_{2p}$ is a function of ω within the accuracy of the data, i. e., the neutron data also appears to scale. If one plots $\nu W_{2p} - \nu W_{2n}$ from this data plus the earlier proton data, then there appears to be a maximum between ω of 3 and 4, at which point $\nu W_{2p} - \nu W_{2n} \approx 0.1$ and the ratio $\nu W_{2n}/\nu W_{2p} \approx 2/3$.

The difference between neutron and proton inelastic scattering is direct evidence for an isospin dependent and therefore non-diffractive (i. e., not due to Pomeron exchange in the language of Regge theory) component of the virtual photon-nucleon scattering amplitude⁸. Another piece of evidence for such a non-diffractive part lies in the behavior of νW_2 and W_1 for large ω (say $\omega > 10$). Since at large ν and

fixed q^2 , $\nu W_2 \propto q^2 (\sigma_T + \sigma_S)$, one would expect νW_2 to fall with increasing ν at fixed q^2 if there is such a non-diffractive component. Unfortunately, there is no separation of νW_2 and W_1 for $\omega \gtrsim 10$ (nor are there data available with large values of q^2 for $\omega > 10$), and therefore one cannot even say for sure that there is scaling in this region. If we use the same small value of R found for $\omega < 10$, then the data are consistent with a scaling behavior and νW_2 decreasing for large values of ω . Alternately, one can consider directly the values of σ_T at points (Table III of reference 2) where a separation has been made and presented at Kiev. One then finds that σ_T appears to be a maximum between ω of 3 and 4 and at $q^2 = 1.5 \text{ GeV}^2$ falls at least as much with increasing energy as the total photo-absorption cross section does over the same ν (or W^2) range as at $q^2 = 0$. Thus, with reasonable assumptions it does appear that νW_2 and σ_T do fall with increasing ω , but exactly how much is beyond the ability of present accelerators to establish.

Some of the striking aspects of the data discussed above, particularly the scaling behavior and point-like magnitude of the data, arise naturally in the parton model.⁹ In this model one considers the electron-nucleon scattering as taking place in an infinite momentum frame at very large ν and q^2 and the electron is assumed to scatter instantaneously and incoherently off point constituents (partons) of the proton. With these assumptions one finds⁹

$$\nu W_2(\nu, q^2) = \sum_N P(N) \sum_{i=1}^N Q_i^2 x f_{Ni}(x) = F_2(x=q^2/2m\nu) \quad (7)$$

where $P(N)$ is the probability of N partons, Q_i is their charge, and $f_{Ni}(x)$ is their longitudinal momentum distribution in terms of the fraction, $x = 1/\omega$, of the total longitudinal momentum of the nucleon which they carry in the infinite momentum

frame. Clearly, since F_2 is a function only of $x = 1/\omega$ in Eq. (7), we have the scaling behavior. The point-like magnitude has been put in through the assumption of point constituents.

Several sum rules follow from Eq. (7). If we assume the same momentum distribution for each of the N partons, then

$$\int_0^1 dx_i x_i f_{Ni}(x_i) = 1/N, \quad (8)$$

and the sum rule

$$\int_0^1 F_2(x) dx = \sum_N P(N) \sum_{i=1}^N \frac{Q_i^2}{N} \quad (9)$$

for the mean squared parton charge follows. Partons with $Q_i = \pm 1$ of course yield $\sum_{i=1}^N Q_i^2/N = 1$, while for a proton with three quarks as partons, $\sum_i Q_i^2/3 = 1/3$, and a quark-antiquark sea with equal amounts of $p\bar{p}$, $n\bar{n}$, and $\lambda\bar{\lambda}$ quarks gives $\sum_i Q_i^2/N = 2/9$. Experimentally²

$$\int_{0.1}^1 dx F_{2p}(x) \approx 0.14 \quad (\pm 15\%) \quad (10)$$

$$\int_{0.1}^1 dx F_{2n}(x) \approx 0.10$$

from the values of $F_2(\omega)$ constructed with the small angle (6° and 10°) data. The large angle data (with larger values of q^2) and/or using ω' to construct F_2 from the small angle data yield slightly smaller values for $\int_0^1 dx F_{2p}(x)$. Since $\int_0^{0.1} dx F_2(x)$, although unmeasured, with any reasonable extrapolation of F_2 to $x=0$ is less than about 0.03, we see that $\int_0^1 F_{2p}(x)dx$ and $\int_0^1 F_{2n}(x)dx$ are too small

to agree with either the simple three quark or quark-antiquark sea model. One is forced to either disregard the sum rule because an assumption used in its derivation is wrong (e. g. , on the same momentum distribution for each parton), or to invoke the presence of neutral partons in addition to the charged ones in order to lower the mean square charge below 2/9. In the first case the sum rule is incorrect, and in the second case it leads to ad hoc models with neutral partons to patch up the discrepancy with experiment. Either way the parton model suffers a loss in predictive power.

The assumption on the momentum distribution does not enter the sum rule

$$\int_0^1 \frac{dx}{x} F_2(x) = \sum_N P(N) \sum_{i=1}^N Q_i^2, \quad (11)$$

which simply follows by integrating Eq. (7) for νW_2 with respect to x and using the normalization condition

$$\int_0^1 dx f_{Ni}(x) = 1. \quad (12)$$

The sum rule (11) was originally proposed by Gottfried¹⁰ in the form

$$\int_0^\infty \frac{d\nu}{\nu} \nu W_2(\nu, q^2) = 1 \quad (13)$$

for the proton (but not the neutron) for all q^2 within the context of the quark model.¹¹ At $q^2 = 0$ this sum rule for the proton is trivially satisfied due to the contribution of the Born term and vanishing (see Eq. (5)) of the continuum. The derivative with respect to q^2 at $q^2 = 0$ of Eq. (13) leads to¹⁰

$$\int_0^{\infty} \frac{d\nu}{\nu} \sigma_T(\nu) = 4\pi^2 \alpha \left[\frac{\langle r^2 \rangle_{F_{1p}}}{3} - \frac{(\mu_p)^2}{4M_N^2} \right] \approx 420 \mu b, \quad (14)$$

where $\sigma_T(\nu)$ is the total photon-proton cross section at $q^2 = 0$. If $\sigma_T(\infty)$ is non-zero, the left hand side of Eq. (14) diverges logarithmically (a similar disease affects Eqs. (11) and (13) if $F_2(0)$ or $\nu W_2(\infty, q^2)$ is not zero). The manner in which Eq. (13) is satisfied at $q^2 = 0$ (by the Born term), however, suggests that if we are to make any sense of Eq. (14) the constant part (due Pomeron exchange in Regge language) of the total cross section (or νW_2) corresponding to the diffractive part of forward Compton scattering should not be counted in the sum rule. Rather, we should include only the direct channel resonances and non-diffractive part of the amplitude. Unfortunately, it is difficult and, more importantly, ambiguous to separate an amplitude into "resonant" and "non-resonant" or "non-diffractive" and "diffractive" contributions, particularly at low energies. If we proceed boldly and subtract from $\sigma_T(\nu)$ at high energies the quantity $\sigma_T(\infty) \approx 100 \mu b$ as the constant part of the photon-proton total cross section at high energies¹², then we obtain values¹³ ranging from 400 to 550 μb for the integral on the left hand side of Eq. (14), depending on how we extrapolate the constant part of σ_T at high energies into the low energy region ($W < 2.0$ GeV). Thus, if we interpret Eq. (13) as being a sum rule for the non-diffractive part of the forward Compton amplitude, it appears to be quite possible that the resulting Eq. (14) is satisfied within the rather large ambiguities in defining what is meant by the words "non-diffractive part".

Going to the opposite limit of large q^2 and using the scaling property of νW_2 , Eq. (13) goes over to Eq. (11) with the right hand side equal to 1 in the simple three quark model.¹¹ Experimentally, we have that²

$$\int_{1/12}^1 \frac{dx}{x} F_{2p}(x) = 0.58 \quad (\pm 10\%) \quad (15)$$

from the 6° and 10° data. Again, a finite value of $F_2(x)$ at $x = 0$ (i. e., ω or $\nu = \infty$) leads to a logarithmically divergent integral, and if we interpret Eq. (13) as discussed above we must again somehow extract the non-diffractive part of the amplitude. This is impossible to do without more complete data for large values of ω . We note, however, that it is possible to obtain the value of l given in Eq. (13) for $\int_0^1 \frac{dx}{x} F_{2p}(x)$ with a suitable non-diffractive component of $\nu W_{2p} = F_{2p}$ above $\omega = 12$ (below $x = 1/12$). Then a large part of the observed F_{2p} both above and below $\omega = 12$ would have to be non-diffractive in character, something which the present data doesn't disagree with, but doesn't necessarily show to be true either. In summary, it is possible for a suitably interpreted version of Eq. (13) to be true from $q^2 = 0$ to ∞ , but it is difficult to give an unambiguous definition of the part of νW_{2p} which is to be included in the sum rule.

The question of extracting a particular component of the amplitude is avoided if we consider

$$\int_0^1 \frac{dx}{x} \left[F_{2p}(x) - F_{2n}(x) \right], \quad (16)$$

because the constant part of $F_2(x)$ as $x \rightarrow 0$ or $\omega \rightarrow \infty$ presumably cancels between the proton and neutron. In a model where the nucleon is made of three quarks or three quarks plus any number of neutral partons (the same neutral partons or quark-antiquark sea for both) the integral in (16) should equal $1/3$. Experimentally²

$$\int_1^{12} \frac{d\omega}{\omega} [F_{2p}(\omega) - F_{2n}(\omega)] = \int_{1/12}^1 \frac{dx}{x} [F_{2p}(x) - F_{2n}(x)] = 0.13 (\pm 40\%). \quad (17)$$

A reasonable form (e. g., $\text{const.}/\omega^{1/2}$) for $F_{2p} - F_{2n}$ for large ω (small x) could make the integral from 0 to 1 in x (1 to ∞ in ω) equal to 1/3, although it requires pushing the values of $F_{2p} - F_{2n}$ to the upper limits of the error bars in the presently available data.²

In brief, while the parton model is an easy way to remember certain features of the data, detailed qualitative comparison of the resulting sum rules⁹ leads to a fairly complicated picture. If taken seriously, sum rules of the form $\int_0^1 dx F_2(x)$ indicate the need for neutral partons, while those of the form $\int_0^1 \frac{dx}{x} F_2(x)$ in any reasonable quark type parton model¹⁴ indicate the need for a large non-diffractive component to the forward virtual photon-nucleon amplitude both above and below $\omega \simeq 10$. Still, the simplest way to remember the data qualitatively is a parton model in which the nucleon is made of three quarks and a quark-antiquark sea, with possibly some neutral partons.¹⁵

Finally, with regard to sum rules, we note that the Bjorken inequality¹⁶

$$\int_0^{\infty} d\nu [W_{2p}(\nu, q) + W_{2n}(\nu, q^2)] \geq 1/2, \quad (18)$$

which can be rewritten at large q^2 using scaling as

$$\int_1^{\infty} \frac{d\omega}{\omega} (F_{2p} + F_{2n})(\omega) \geq 1/2, \quad (19)$$

is formally satisfied by the data if the upper limit of integration is taken to be at $\omega \simeq 5$. One previously worried that the Bjorken inequality would be trivially

satisfied due to the constant part of $\nu W_2(\nu, q^2)$ as $\nu \rightarrow \infty$ ($F_2(\omega)$ as $\omega \rightarrow \infty$),

which leads to the logarithmic divergence of the integral discussed before.

However, since we now know that between $\omega = 1$ and 5 νW_{2p} is rather different than νW_{2n} , we can have some confidence that most of the integrand in this region of ω is not due to a diffractive part of νW_2 and hence the inequality may well be non-trivially satisfied. Similarly the Adler sum rule¹⁷ for inelastic neutrino scattering,

$$\int_0^\infty d\nu \left[W_2^{(\bar{\nu})}(\nu, q^2) - W_2^{(\nu)}(\nu, q^2) \right] = 1, \quad (20)$$

from which the Bjorken inequality is derived, now can be plausibly argued as being correct, but we shall not know for sure until actual experiments are done with neutrinos and anti-neutrinos.

In our discussion of various sum rules above we have seen the importance to the success of several sum rules in the presence of a large non-diffractive component of the forward Compton amplitude for virtual photons. As noted earlier, direct and unambiguous experimental evidence now exists for at least some non-diffractive, isospin dependent component from the observation of a difference between electron-proton and electron-neutron inelastic scattering. The apparent decrease in νW_2 or $\sigma_T(\nu, q^2)$ for large ω or ν is also evidence for such a component. Such a non-diffractive component of a forward amplitude and the corresponding decreasing total cross section at high energy is correlated with the presence and behavior of resonances at low energy, at least for purely hadronic processes. This correlation is part of the more general concept of duality and takes quantitative form in terms of finite energy sum rules.¹⁸

Thus we might guess that the resonances, and in particular those resonances that give rise to prominent bumps in the total cross section, could have a behavior which is correlated with other features of inelastic electron scattering.¹⁹ In particular, we would like to compare the behavior of the resonances to the behavior of νW_2 and W_1 in the scaling limit where ν and $q^2 \rightarrow \infty$. In the study of the behavior of the resonances, the variable ω' introduced previously, which results in νW_2 and W_1 exhibiting scaling for smaller values of q^2 , has an additional advantage. If νW_2 is considered as a function of ω , the resonances occur at values of $\omega > 1$, with any particular resonance moving toward $\omega = 1$ as q^2 increases. On the other hand, the nucleon pole term in νW_2 , corresponding to elastic scattering, always occurs at $\omega = 1$. With respect to $\omega' = 1 + W^2/q^2$, however, the nucleon and all other resonances all occur at values of $\omega' > 1$ and move toward 1 as q^2 increases. The nucleon is then not treated in a special way compared to other resonances. As we will shortly see, this also allows one to understand in another way the connection found²⁰ in the parton model between the behavior of the elastic form factors and of νW_2 as $\omega \rightarrow 1$.

The behavior of the resonances in comparison to νW_2 in the scaling limit can be seen¹⁹ in Figure 6 where we have plotted the data for νW_2 versus ω' (assuming $R = \sigma_S/\sigma_T = 0$). The dashed line, which is the same in all cases, is a smooth curve through the high energy 10^0 data²¹ in the region beyond the prominent resonances ($W > 2.0$ GeV) and with large q^2 ($3 < q^2 < 7$ GeV²).²² We call this dashed line, therefore, the "scaling limit curve" $\nu W_2(\omega')$. The solid lines are smooth curves through the 6^0 data at various incident energies. As the incident energy E increases, so does q^2 and the resonances and elastic peak move toward $\omega' = 1$.

We note two important things from Figure 6. First, as similar graphs of the 10^0 data in the resonance region also show²³, the prominent resonances do not disappear at large q^2 relative to a "background" under them which has the scaling behavior. Secondly, as q^2 changes the prominent resonances roughly follow in magnitude the scaling limit curve. Thus, both the prominent resonances and any "background" have a behavior as q^2 changes which is closely correlated with the scaling behavior of νW_2 . Note that the ratio of height of resonance peak to background and the correlation of resonance peak height to the scaling limit curve could be seen if we plotted the data with respect to other variables (in particular, ω). However, in addition to not showing the onset of scaling behavior for $W > 2$ GeV at smaller values of q^2 , the other plots often require very careful inspection to see these relevant features of the data, while ω' plots allow one to see it at a glance.²⁴

Thus, at least the prominent resonances do not seem to be a separate entity with a behavior divorced from that of the rest of the data, but instead appear to be an intrinsic part of the scaling behavior. One of course cannot determine without a detailed partial wave analysis of the hadronic final state exactly what the many broad, low spin N^* resonances that we know exist are doing as a function of q^2 . But the behavior of the prominent N^* 's that we can see gives us the clue to what is happening. Using the duality framework²⁵, we would say that the nucleon and other resonances at low energy build (in the sense of finite energy sum rules) the relevant non-Pomeron exchanges at high energy, which will result in a falling $\sigma_T(q^2, \nu)$ or νW_2 curve and a difference between νW_{2p} and νW_{2n} .

What is unique to studying duality in electroproduction is the experimentally observed scaling behavior. This allows us to consider data at fixed values of ω'

but different values of q^2 and W^2 , both within and outside the region of prominent resonances. Thus we can compare the data where there are prominent narrow resonances directly with data for $\nu W_2(\omega')$ for large q^2 and W^2 where nature has accomplished the appropriate averaging of the many broad resonances and background present there. One can give this comparison quantitative form²⁶ in terms of finite energy sum rules where we find that $\nu W_2(\omega')$ acts as a smooth averaging function for $\nu W_2(\nu, q^2)$, i. e., the area under $\nu W_2(\nu, q^2)$ should be the same as that under the scaling limit curve $\nu W_2(\omega')$ if we integrate at fixed $q^2 \gtrsim 1 \text{ GeV}^2$ up to a value of ν or ω' above which the scaling behavior, $\nu W_2(\nu, q^2) = \nu W_2(\omega')$, is true.

In spite of the existence of explicit models²⁷ of the structure functions as sums of resonances, there has been a point of confusion as to how resonances, which are known to have excitation form factors which fall rapidly with increasing q^2 , can be consistent with the "deep inelastic" data which is supposed to be characterized by a slow q^2 variation. The confusion results from the fact that the "deep inelastic" data exhibit (for fixed W , say) more than one q^2 dependence. If $1 + W^2/q^2$ corresponds to an ω' which is larger than ≈ 5 , $\nu W_2(\omega')$ varies very slowly and $\sigma_T \propto (1/q^2)\nu W_2 \propto 1/q^2$; but if $1 + W^2/q^2$ corresponds to $\omega' \lesssim 3$, then $\nu W_2(\omega')$ varies rapidly with ω' and hence with q^2 at fixed W . Thus the cross section at say $W = 3 \text{ GeV}$ should start falling as $1/q^2$ for small q^2 , but when $q^2 \gtrsim 4 \text{ GeV}^2$, so that we are below the knee of the νW_2 curve, σ_T should fall much faster. We can put this in quantitative form as follows: if $G(q^2)$ is the excitation form factor of the hadronic final state of mass W and

$$G(q^2) \rightarrow c(1/q^2)^{n/2} \quad (21)$$

as $q^2 \rightarrow \infty$, while νW_2 can be parametrized as

$$\nu W_2(\omega') \rightarrow c'(\omega' - 1)^p \quad (22)$$

as $\omega' \rightarrow 1$, then we must have

$$n = p + 1. \quad (23)$$

Thus each hadronic final state of mass W , if it is to participate in the scaling behavior, must have an excitation form factor with the same power of fall-off in q^2 as $q^2 \rightarrow \infty$, and this power is related to the power with which νW_2 rises at threshold. If we apply this in the low energy region to a given resonance of mass W_R (including the nucleon) we see that all resonances which follow $\nu W_2(\omega')$ in magnitude must have the same power of fall off in q^2 as $q^2 \rightarrow \infty$ (including the elastic with $n \simeq 4$), and again this is related to the behavior of νW_2 at threshold. Eq. (23) for the case of the elastic peak is just the relation of Drell and Yan²⁰ first found in the parton model.

The rather local averaging of the resonances by $\nu W_2(\omega')$ seen in Figure 6 encourages one to go further and make the very strong assumption that at large q^2 the elastic contribution to νW_2 is averaged in the sense of finite energy sum rules by $\nu W_2(\omega')$. Specifically, one assumes that the area under the elastic peak (delta function) in νW_2 is the same as the area under the scaling limit curve $\nu W_2(\omega')$ from $\omega' = 1$ to an ω' corresponding to a hadron mass $W = W_t$ near physical pion threshold. This allows¹⁹ one not only to again establish the connection (23) between the elastic form factor's behavior as $q^2 \rightarrow \infty$ and the behavior of νW_2 near $\omega' = 1$, but also allows a quantitative calculation of νW_2 near $\omega' = 1$ from elastic scattering data.²⁸ Furthermore, the same assumption also predicts from the behavior of the

elastic form factors that $R = \sigma_S/\sigma_T \rightarrow 0$ as $q^2 \rightarrow \infty$ and $\omega' \rightarrow 1$, as well as $\nu W_{2n}/\nu W_{2p} \rightarrow (\mu_n/\mu_p)^2 = 0.47$ in the same limit. As can be seen from Figure 5, the 6° and 10° data seem to show this last prediction is not far from the truth, but only the large angle deuterium data to be taken soon at SLAC will go to small enough values of ω' to really tell if this is true.

There are many other interesting aspects of inelastic electron-nucleon scattering and related processes which unfortunately cannot be discussed in this talk, but which are of great importance and will be discussed by others at this Symposium. As already noted, the observation of a difference between electron-proton and electron-neutron inelastic scattering makes it very likely that neutrino and anti-neutrino inelastic scattering are also different. One should also expect non-zero asymmetries in the scattering of polarized electrons or muons on polarized protons, something which will likely be investigated experimentally in the near future. Slightly further afield is the behavior of the cross section for $e^- + e^+ \rightarrow$ hadrons. The observation at Frascati of large (i. e., point-like) cross sections is very exciting and again indicates the possible relevance of parton ideas. Such ideas may also be relevant in studying the behavior of muon pair production in hadron-hadron collisions.²⁹

Altogether, the last few months have seen some real progress in inelastic scattering both experimentally and theoretically. Furthermore, I think that our theoretical progress has not all been of the negative kind, i. e., the elimination of some of the proposed theories and models. We not only have direct experimental evidence for the presence of a substantial non-diffractive, isospin dependent component of the forward Compton amplitude for virtual photons but I think we have a much more unified understanding of the relation between the behavior of the

elastic form factors and the threshold behavior of νW_2 , the behavior of the resonance excitation and the scaling behavior, etc. However, we still do not have a detailed quantitative theory which does more than relate one kind of observed behavior to another. Perhaps this should be no surprise, since such a quantitative theory would probably have to come quite close to being a complete theory of strong interactions and of the composition of hadrons.

References

1. For a review of the experimental and theoretical situation as of a year ago, see the invited talks of R. E. Taylor and F. J. Gilman in Proceedings of the Fourth International Symposium on Electron and Photon Interactions at High Energies, Liverpool, 1969.
2. E. D. Bloom et al., "Recent Results in Inelastic Electron Scattering", SLAC-PUB-796, report presented to the XVth International Conference on High Energy Physics, Kiev, USSR (1970).
3. See in particular the talk of C. H. Llewellyn Smith, "An Introduction to Highly Inelastic Lepton Scattering and Related Processes", CERN TH-1188, July 1970.
4. L. N. Hand, Phys. Rev. 129, 1834 (1963). For the connections between the various amplitudes and the kinematics of inelastic scattering see F. J. Gilman, Phys. Rev. 167, 1365 (1968).
5. J. D. Bjorken, Phys. Rev. 179, 1547 (1969).
6. More generally, we have $\omega' = (2M_N\nu + m^2)/q^2 = \omega + m^2/q^2$ where m has the dimensions of a mass. Clearly, $\omega' \rightarrow \omega$ as $q^2 \rightarrow \infty$. We have taken $m = M_N$ in Eq. (6), which, aside from its simplicity, is consistent with the value $m^2 \simeq 0.9 \text{ GeV}^2$ obtained in a best fit² to the data for νW_2 .
7. Given the size of the presently quoted errors one cannot determine if ω or ω' plots are better for $\nu W_{2n}/\nu W_{2p}$.
8. Recall the connection between the imaginary part of the forward Compton amplitude for photons of $(\text{mass})^2 = -q^2$ and the structure functions W_1 and W_2 given in Eq. (4). When we discuss the "non-diffractive component" in the following we shall always be referring to that part of the forward Compton amplitude which is not due to Pomeron exchange in the language of Regge

theory and which leads to a falling part of total cross sections at high energy. It is interesting that the high energy γn and γp total cross sections at $q^2 = 0$ as analyzed in D. O. Caldwell et al., Phys. Rev. Letters 25, 613 (1970) have non-diffractive parts (i. e., the parts falling with energy) which are approximately in the ratio 2/3. This is precisely the ratio expected in the quark model for "deep inelastic" scattering, corresponds to $I = 0$ and $I = 1$ exchanges in Compton scattering with pure F-type coupling at the baryon vertex, and equals $\nu W_{2n} / \nu W_{2p}$ between ω of 3 and 4, where $\nu W_{2p} - \nu W_{2n}$ is a maximum.

9. R. P. Feynman, Phys. Rev. Letters 23, 1415 (1969) and unpublished lectures. J. D. Bjorken and E. A. Paschos, Phys. Rev. 185, 1975 (1969).
10. K. Gottfried, Phys. Rev. Letters 18, 1174 (1967).
11. The possible correlation terms vanish in the quark model for the proton, but not the neutron (see ref. 10). At large q^2 the correlation terms for both the neutron and proton vanish, and, using the scaling behavior of νW_2 , Eq. (13) goes over to Eq. (11) with 1 on the right hand side for the proton and 2/3 for the neutron if we take the quark model for the nucleon to calculate $\sum_i Q_i^2$ in Eq. (11).
12. M. Damashek and F. J. Gilman, Phys. Rev. D1, 1319 (1970).
13. F. J. Gilman, unpublished.
14. One is already fairly restricted also by the small measured values of $R = \sigma_S / \sigma_T$, which demand the dominance of spin $\frac{1}{2}$ charged partons, and by the deviation of $\nu W_{2n} / \nu W_{2p}$ from unity, which demands different charged partons in the proton and neutron, i. e., the existence of some non-diffractive component.

15. Such models have been recently discussed by K. Kitani and H. Yoshii, Tokyo Institute of Technology preprints, July 1970 (unpublished).
16. J. D. Bjorken, Phys. Rev. Letters 16, 408 (1966).
17. S. L. Adler, Phys. Rev. 143, 1144 (1966).
18. See R. Dolen, D. Horn, and C. Schmid, Phys. Rev. 166, 1768 (1968); H. Harari, Phys. Rev. Letters 20, 1395 (1968); P. Freund, Phys. Rev. Letters 21, 235 (1968); F. J. Gilman, H. Harari and Y. Zarmi, Phys. Rev. Letters 21, 323 (1968).
19. E. D. Bloom and F. J. Gilman, Phys. Rev. Letters 25, 1140 (1970).
20. S. D. Drell and T. M. Yan, Phys. Rev. Letters 24, 181 (1970). See also G. West, Phys. Rev. Letters 24, 1206 (1970).
21. E. D. Bloom et al., Phys. Rev. Letters 23, 930 (1969). M. Breidenbach, MIT thesis, 1970 (unpublished).
22. The actual data points from both the small and large angle data used in constructing $\nu W_2(\omega')$ can be seen in Figure 4.
23. See also the prominent resonance peaks in $\sigma_T + \epsilon \sigma_S$ at $q^2 = 0, 1, 2$ and 4 GeV^2 in Figure 9 of R. E. Taylor, reference 1.
24. Aside from the scaling behavior which gives an additional reason for preferring ω' rather than ω , the choice between ω' and ω for plotting the data is somewhat similar to the choice between ν and s to extrapolate high energy Regge pole fits into the low energy region. Although an extrapolation using s instead of ν in the forward amplitude for pion-nucleon charge exchange results in a much poorer averaging of the low energy resonances, this doesn't change the physics, i. e., that the sum of the resonance contributions to the amplitude suitably averaged is equal to the Regge pole amplitude and the two should not be added to one another. Similarly here, one may get a better or worse local averaging using a different variable, but it doesn't change the physics of the correlation between the behavior of resonance excitation and the scaling behavior.

25. This application of duality ideas to inelastic electron scattering differs from the previous one of H. Harari, Phys. Rev. Letters 22, 1078 (1969) in the interpretation of the data for resonance electroproduction and the behavior of νW_2 for large ω , aside from the fact that the proposal of Pomeron-exchange dominance given in the above paper is ruled out by the difference between electron-proton and electron-neutron inelastic scattering.
26. See Eq. (1) and the discussion following it in E. D. Bloom and F. J. Gilman, reference 19.
27. See in particular the Veneziano-like model of P. V. Landshoff and J. C. Polkinghorne, Nuclear Phys. B19, 432 (1970) and the work of G. Domokos and S. Kovési-Domokos, Johns Hopkins University preprint, 1970 (unpublished).
28. The calculated $\nu W_2(\omega')$ curve for $1 < \omega' < 1.5$, using an appropriate choice of W_t , averages the data in the resonance region of the highest energy (17.7 GeV) 10^0 data and appears to agree also with the scaling limit curve which results from the analysis of the large angle data with $W > 2$ GeV. See reference 19. Also see the talk of M. Nauenberg at this Symposium on finite energy sum rules to construct $\nu W_2(\omega)$.
29. Some of these subjects are covered in the talks at this Symposium by Drs. Kuti, Galfi, Kunszt, Sartori, and Brandt.

Figure Captions

- Figure 1 Kinematics of inelastic electron-nucleon scattering.
- Figure 2 Values of νW_2 at fixed $\omega = 4$ and various values of q^2 .
- Figure 3 Values of νW_2 versus $\omega = 2M_N \nu / q^2$ for data with $W > 2$ GeV and various ranges of q^2 (in GeV^2).
- Figure 4 Values of νW_2 versus $\omega' = 1 + W^2 / q^2$ for data with $W > 2$ GeV and various ranges of q^2 (in GeV^2).
- Figure 5 Values of $(D/H-1)$ plotted versus ω . All data points have $q^2 \geq 1 \text{ GeV}^2$. Assuming $R = \sigma_S / \sigma_T$ is the same for neutron and proton and neglecting deuterium corrections (which should be small), the ordinate is $\nu W_{2n} / \nu W_{2p}$.
- Figure 6 The function νW_{2p} plotted versus $\omega' = (2M_N \nu + m^2) / q^2$ with $m^2 = M_N^2$. The solid lines are smooth curves drawn through the $\theta = 6^\circ$ data at various incident energies. The dashed curve, which is the same in all cases, is a smooth curve through large ν and q^2 data. All data is plotted assuming $R = \sigma_S / \sigma_T = 0$. The $E = 7$ GeV data involves values of q^2 all of which are considered outside the scaling region.

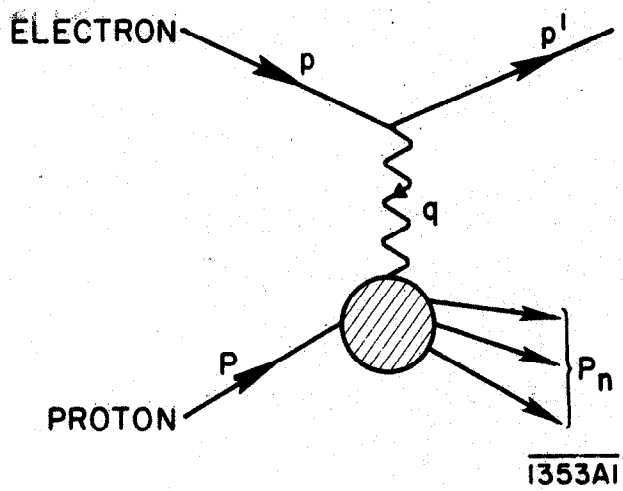


Fig. 1

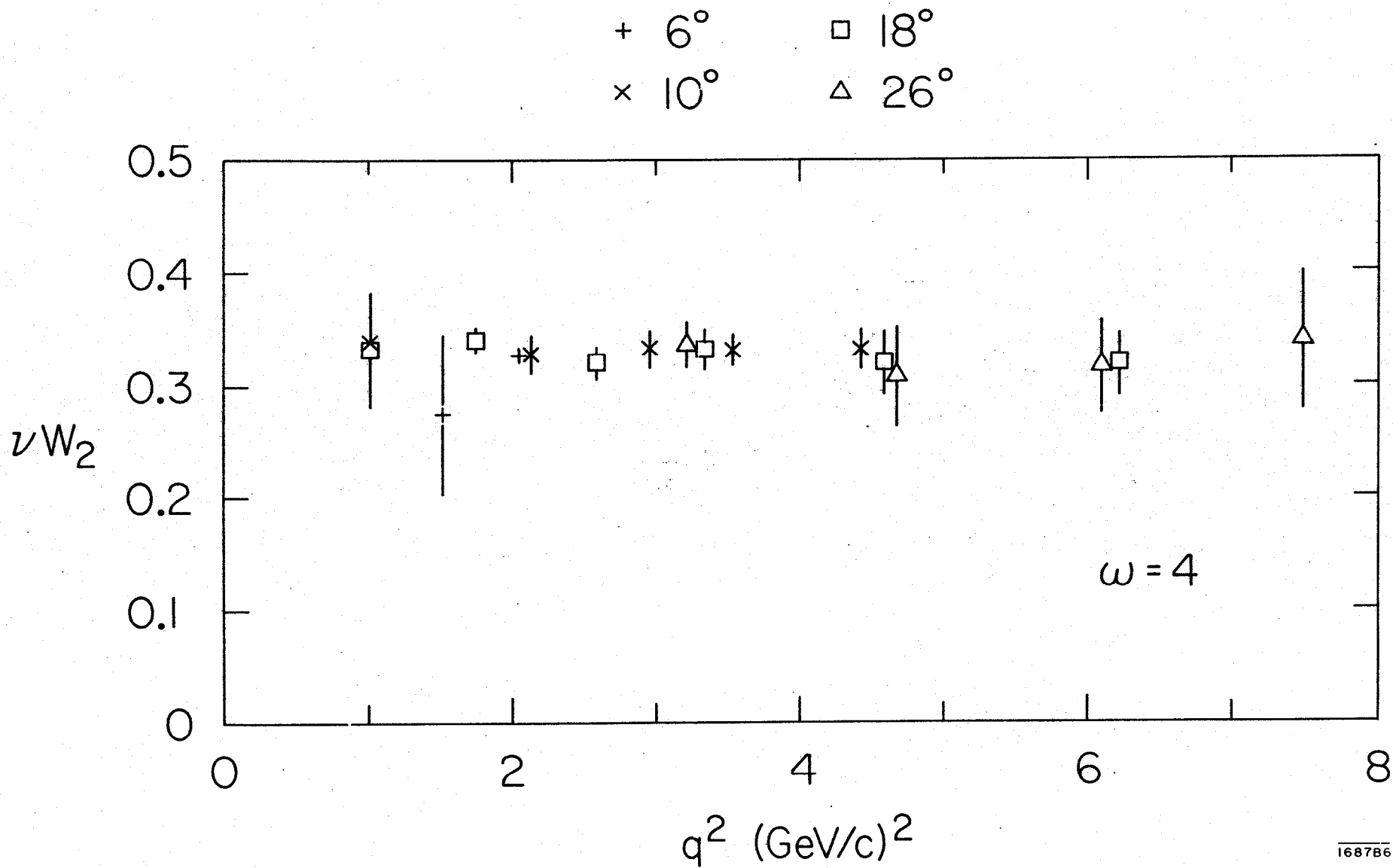


Fig. 2

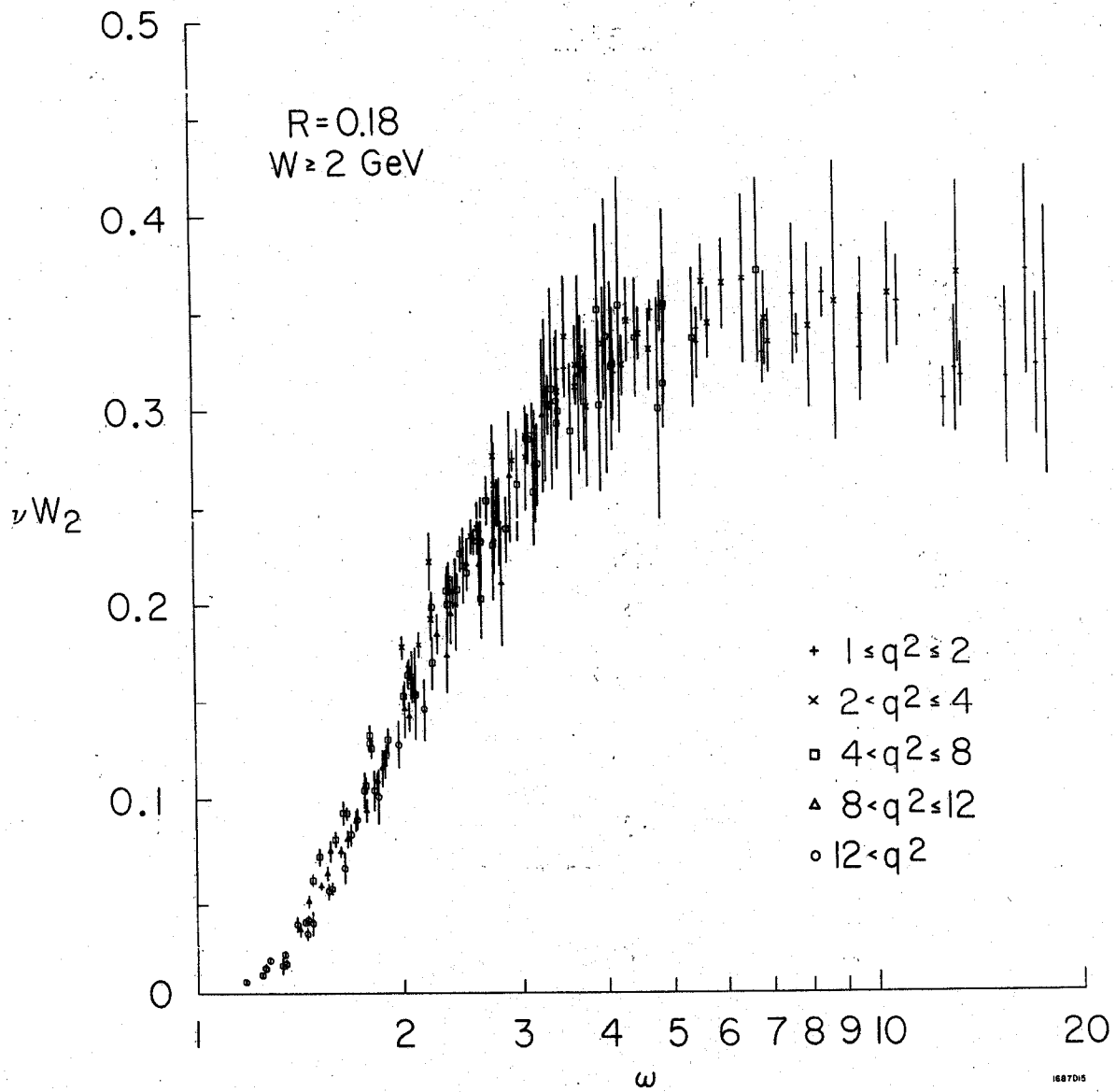


Fig. 3

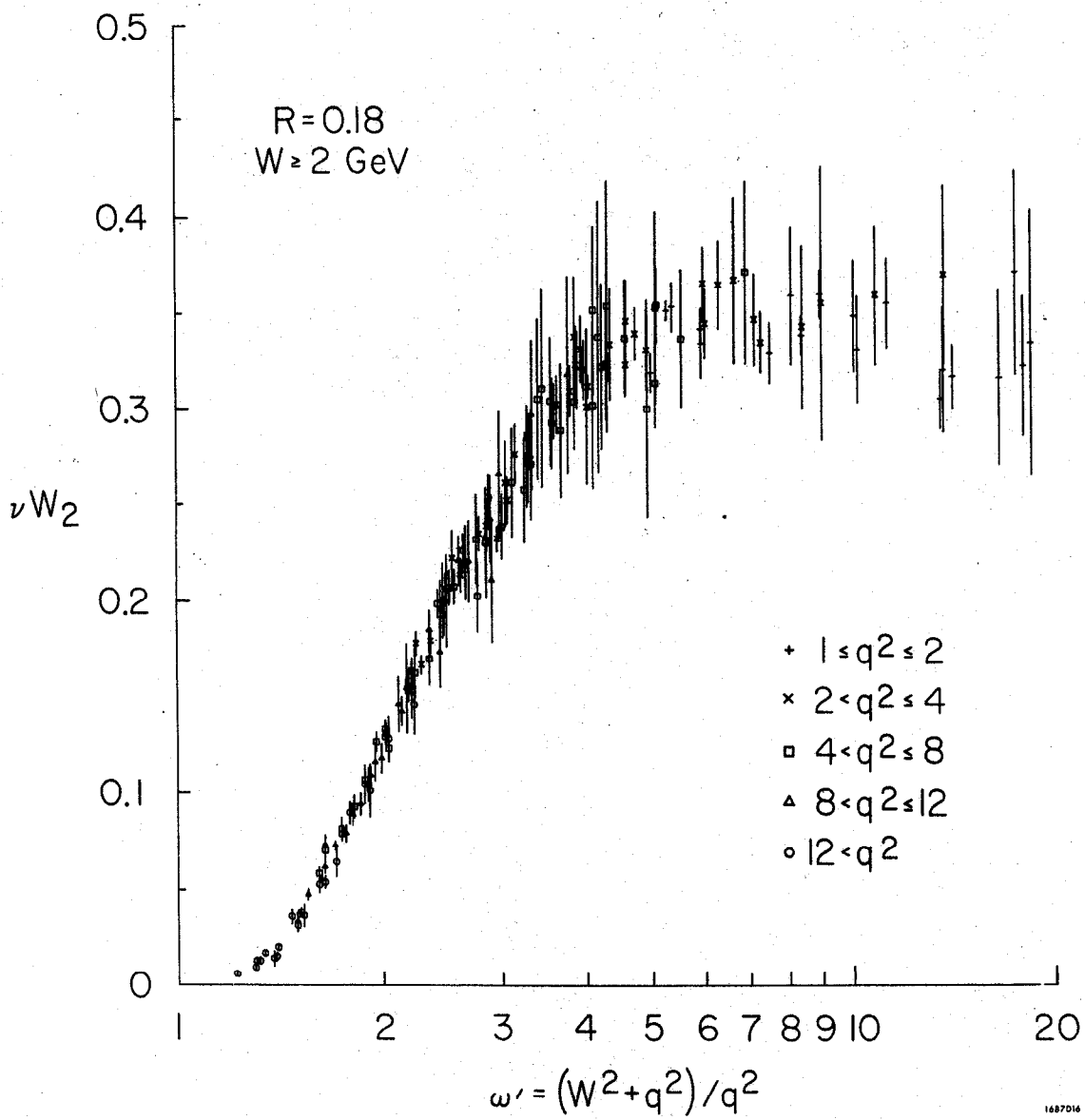


Fig. 4

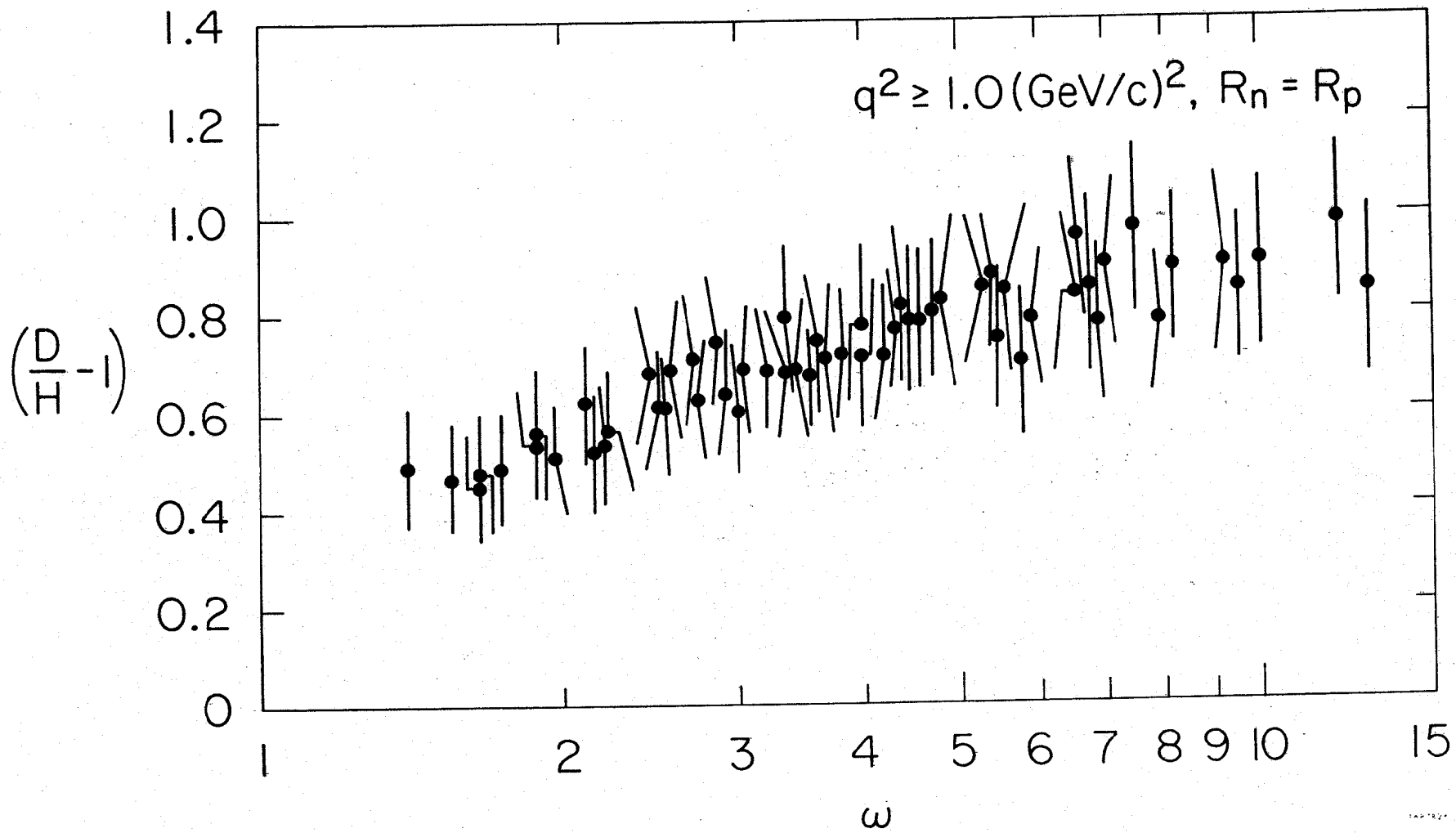


Fig. 5

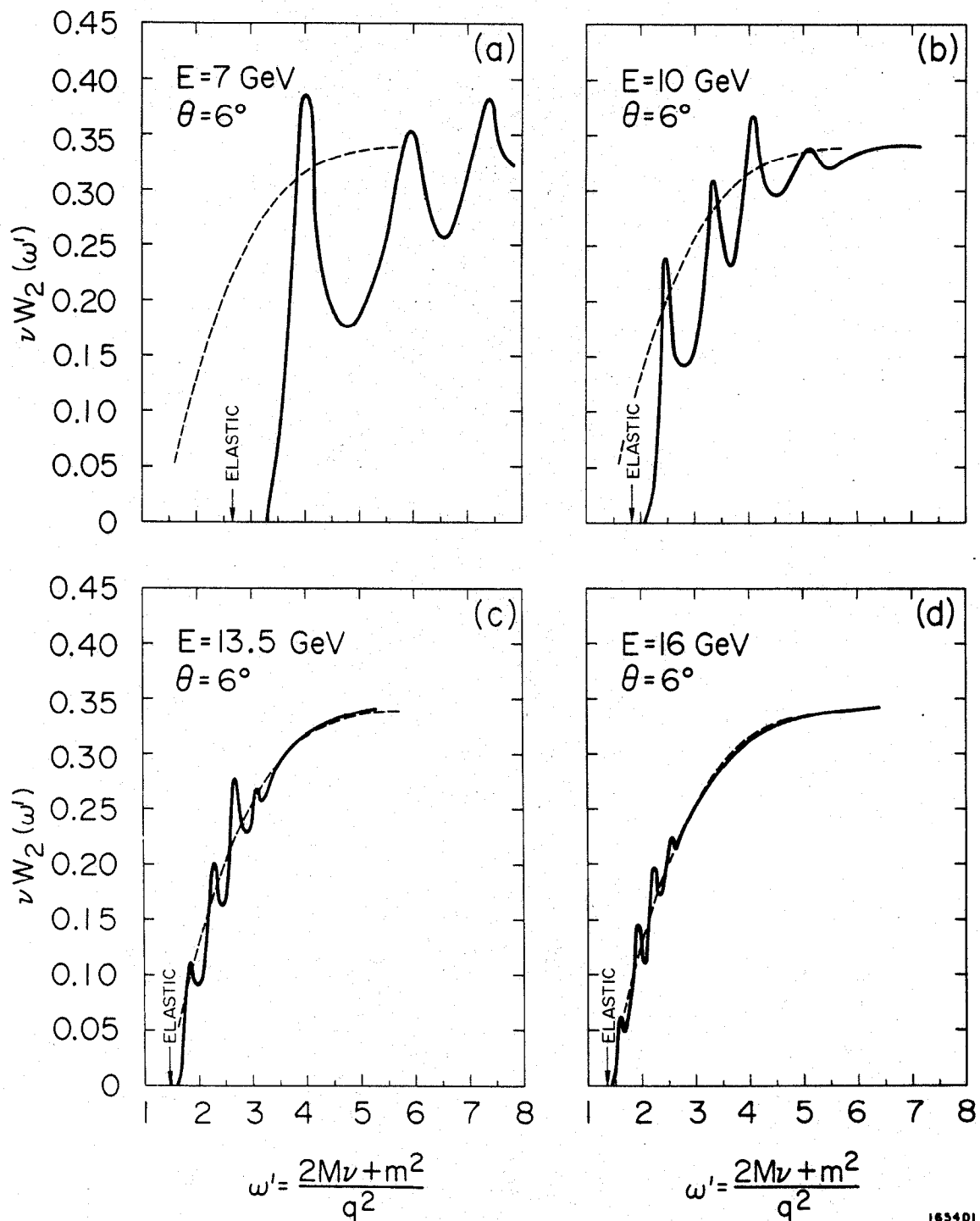


Fig. 6